# Current Distribution on PEM Fuel Cells with Different Flow Channel Patterns

André L. R. Paulino[1]*, Eric Robalinho[2], Edgar F. Cunha[1], Raimundo R. Passos[3] and Elisabete I. Santiago[1]

[1] Instituto de Pesquisas Energéticas e Nucleares IPEN/CNEN-SP, São Paulo, Brazil
[2] Universidade Nove de Julho UNINOVE, São Paulo, Brazil
[3] Universidade Federal do Amazonas UFAM, Manaus, Brazil
*Corresponding author: Av. Prof. Lineu Prestes 2242 – Cidade Universitária, 05508-000 São Paulo-SP, Brazil. Email: andrelrpaulino@usp.br

**Abstract:** In this paper, PEM fuel cells with serpentine and interdigitated flow channel patterns were studied. The main objective was to analyze the influence of the flow channel design in the current distribution over the cell. A 3D isothermal model comprising the entire 5 cm² cell was developed for this study. Polarization curves show that both cells have very similar performances. However, current density plots indicate major differences between them. In the serpentine pattern, current generation is concentrated near the gas entrance, while in the interdigitated pattern, current densities are more distributed over the cell area.

**Keywords:** PEMFC, Channel patterns, Serpentine, Interdigitated, Current distribution

## 1. Introduction

Fuel cells are among the most important technologies for efficient energy generation. These electrochemical devices convert chemical energy directly into electricity. Proton exchange membrane fuel cells (PEMFCs) are especially attractive, due to their low operating temperature and suitability for use in several applications, such as stationary or mobile power generation.

The main components of a PEMFC are the membrane-electrode assembly (MEA) and bipolar plates. The MEA can be considered the core of the fuel cell, since chemical reactions and electric generation occur on it. Bipolar plates (or monopolar plates in unitary cells) are responsible for mechanical support, electric contact with the external circuit and supply of reactants over the MEA. These plates are engraved with channels, through which fuel and products flow [1].

In an electrochemical reaction, current is proportional to the reaction rate, which, in turn, depends on the concentration of reactants. It is important that current be uniform throughout the plane parallel to the MEA, since current distribution and resulting Joule effect can influence the fuel cell heat and water managements. The flow channel pattern influences fuel concentration throughout the cell, and may lead to an irregular current distribution. This may be of minor impact in small cells, but must be considered in larger stacks. Heat generation due to electric current, the Joule effect, is more intense in high current densities, consequently making some regions hotter than others. In colder regions, water condensation is more likely, which causes flooding in the channels and greatly affects fuel cell performance.

In general, parallel, serpentine and interdigitated flow channel patterns in monopolar plates are studied for fuel cell systems. Previous studies have reported problems associated to parallel plates [2,3] compared to the others, therefore only serpentine and interdigitated patterns (Figure 1) will be compared in this work.
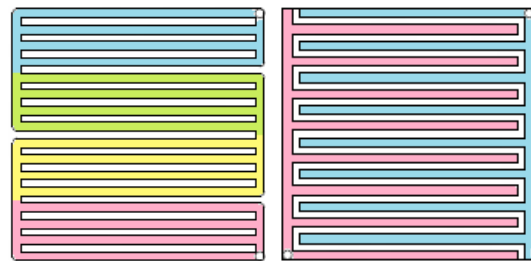


**Figure 1.** Serpentine (left) and interdigitated (right) flow channel patterns

In the serpentine pattern, species are transported from the channel through the gas diffusion layer and into to the catalyst layer and vice-versa mainly by diffusion, while the gas flows along the channels. The flow path in this pattern is continuous, which eliminates areas of stagnant flow, however reactant depletion along

the channel may lower downstream performance [4].

In the interdigitated pattern, the flow field is not continuous, and the channels are either connected to the inlet or the outlet, alternately. This forces the gas to flow over the ribs and through the electrode, causing forced convection and enhancing species transport and facilitating water removal. Nevertheless, this flow pattern causes a much higher pressure drop than its serpentine counterpart, as the gas must flow through the porous layer [5].

## 2. Model Description

The 3D model used in this study (shown in Figure 2 and Figure 3 encompass entire 5 cm² fuel cells, similar to actual prototypes under tests in the laboratory. The plates have 16 flow channels with width of 0.8 mm, intercalated with 0.65 mm ribs [6]. The meshes constructed are completely structured, composed exclusively of hexahedral elements (Figure 3). The meshes consist of 506k elements, and 448k elements for the serpentine and interdigitated models, respectively.
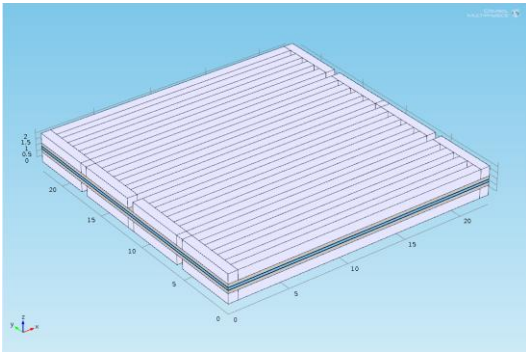


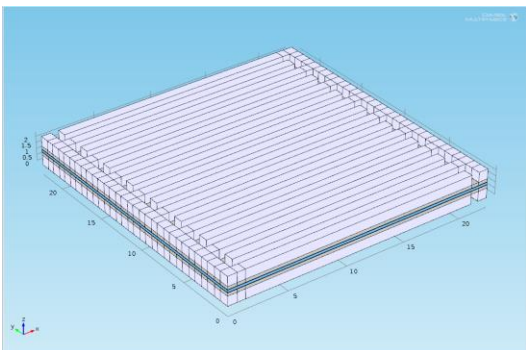**Figure 2.** Geometry built for the serpentine model



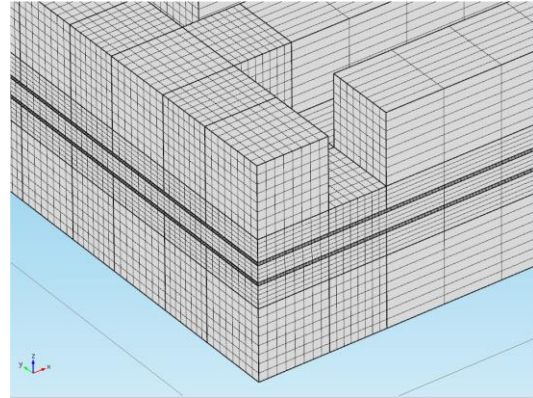**Figure 3.** Geometry built for the interdigitated model



**Figure 4.** Mesh detail for the interdigitated model

As a simplification, the system is isothermal and all chemical species are considered ideal gases. The cell operates in steady-state, the flow is laminar (low Reynolds number) and all materials properties are homogeneous. Humidified hydrogen and oxygen (both with 40% m/m of vapor) are used as feed [7].

In the mathematical model, the following conservation and reaction equations were used:

1. Butler-Volmer equation for the reaction in the anodic catalyst layer;
2. Tafel equation for the reaction in the cathodic catalyst layer;
3. Ohm's law for the ionic and electronic charge transport;
4. Navier-Stokes equations for the free flow in the channels;
5. Brinkman equations for the flow in porous layers;
6. Maxwell-Stefan equations for chemical species transport in the gas phase.

Electrochemical reactions and charge transport were modeled using the Secondary Current Distribution interface. Free and Porous Media Flow interface was used for modeling momentum transport. Diffusion of reactants and products was modeled with the Transport of Concentrated Species interface.

## 3. Governing Equations

The electrochemical reactions in fuel cells are indicated in the equations:

$$H_2 \rightarrow 2H^+ + 2e^-$$

$$\frac{1}{2} O_2 + 2H^+ + 2e^- \rightarrow H_2O$$

$$H_2 + \frac{1}{2} O_2 \rightarrow H_2O$$
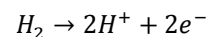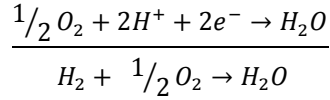
These reactions take place in the electrodes, and their kinetics, responsible for activation overpotential, is described by the Butler-Volmer equation:

$$i = i_o \left[ \exp\left( \frac{-\alpha_R F}{RT} \eta \right) - \exp\left( \frac{\alpha_O F}{RT} \eta \right) \right]$$

where $i$ is the current density, $i_0$ is the exchange current density, $\alpha_R$ and $\alpha_O$ are the transfer coefficients, $T$ is the operating temperature, $F$ and $R$ are the Faraday and the gas constants and $\eta$ is the overpotential.

When the overpotential is high, i.e. such reaction is the rate-determining step [8], which is the case for the cathode, the Butler-Volmer equation is simplified to the Tafel equation:

$$\eta = A \ln\left( \frac{i}{i_0} \right)$$

where $A$ is called Tafel slope.

Charge transport in the electrode and electrolyte is based on Ohm's law, described by:

$$\nabla \cdot \mathbf{i}_k = \mathbf{Q}_k \qquad , \qquad \mathbf{i}_k = -\sigma_k \nabla \phi_k$$

where $\mathbf{i}_k$ is the current density $\mathbf{Q}_k$ is a source term, $\sigma_k$ is the conductivity and $\phi_k$ is the potential, while $k$ denotes an index that is $l$ for the electrolyte and $s$ for the electrode.

In the channels, gas flow is governed by the Navier-Stokes equations for compressible fluids:

$$\nabla \cdot (\rho \mathbf{u}) = 0$$
$$\rho \mathbf{u} \cdot \nabla \mathbf{u} = -\nabla \cdot (-p\mathbf{I} + \tau)$$
$$\tau = \mu [\nabla \mathbf{u} + (\nabla \mathbf{u})^T] - \frac{2}{3} \mu (\nabla \cdot \mathbf{u}) \mathbf{I}$$

where $\rho$ is the density, $\mathbf{u}$ is the velocity vector, $p$ is the pressure, $\tau$ is the viscous stress tensor and $\mu$ is the dynamic viscosity.

In porous media, found in the catalyst and diffusion layers, the Navier-Stokes is changed into the Brinkman equations:

$$\nabla \cdot (\rho \mathbf{u}) = \mathbf{Q}_{br}$$

$$\frac{\rho}{\varepsilon_p} \left[ (\mathbf{u} \cdot \nabla) \frac{\mathbf{u}}{\varepsilon_p} \right] = \nabla \cdot \left( -p\mathbf{I} + \frac{\tau}{\varepsilon_p} \right) - \left( \frac{\mu}{\kappa} + \frac{\mathbf{Q}_{br}}{\varepsilon_p^2} \right) \mathbf{u}$$

where $\mathbf{Q}_{br}$ is a mass source or sink, $\varepsilon_p$ is the porosity and $\kappa$ is the permeability of the porous media.

Chemical species transport in ideal gas mixtures is described by the Maxwell-Stefan equation:

$$\rho(\mathbf{u} \cdot \nabla)\omega_i = \nabla \cdot \left( \rho \omega_i \sum_{k=1}^{Q} \widetilde{\mathbf{D}}_{ik} \mathbf{d}_k \right) + R_i$$

$$\mathbf{d}_k = \nabla x_k + \frac{1}{p} [(x_k - \omega_k)\nabla p]$$

$$x_k = \frac{\omega_k}{M_k} \bar{M} \qquad , \qquad \frac{1}{\bar{M}} = \sum_{i=1}^{Q} \frac{\omega_i}{M_i}$$

where the indexes $i$ and $k$ represent different species, $\rho$ is the mixture density, $\omega_i$ is the mass fraction, $\widetilde{\mathbf{D}}_{ik}$ are the multicomponent diffusivities, $\mathbf{d}_k$ is the diffusional driving force, $R_i$ is the rate of production or consumption, $x_k$ is the mole fraction, $p$ is the total pressure, $M_k$ is the molar mass and $\bar{M}$ is the mean molar mass of the mixture.

## 4. Results

Polarization curves for both patterns were plotted and are shown in Figure 5. The plots show that they behave similarly, and yield almost the same values of potential over all the current density range. Therefore, it is implied that fuel cell performance is not significantly influenced by channel design.
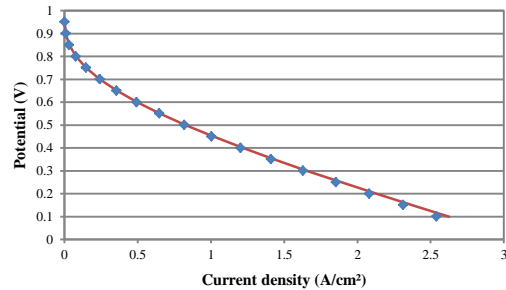


**Figure 5.** Polarization curves for the serpentine (blue dots) and interdigitated (red line) patterns

The main difference between these two patterns is on the regions supplied with a high concentration of reactants. In the serpentine, only the first four channels receive concentrated reactants, while in the last channels they are present in a very low concentration (Figure 6).
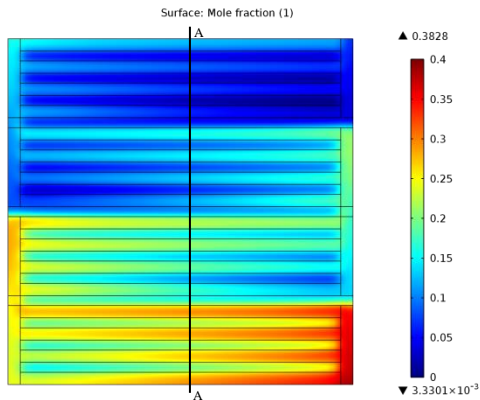


**Figure 6.** Mole fraction of oxygen in the catalyst layer midplane for the serpentine pattern

In contrast, the interdigitated pattern distributes concentrated gas to alternate channels, ensuring reactant distribution over a large area of the fuel cell (Figure 7).
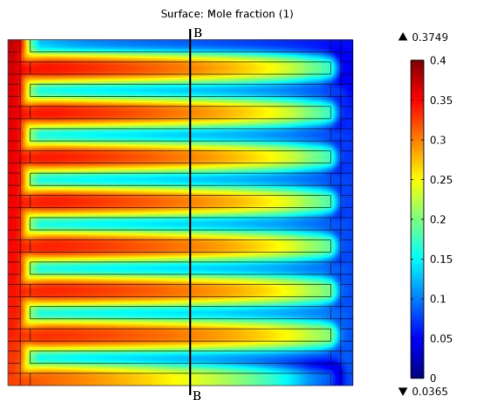


**Figure 7.** Mole fraction of oxygen in the catalyst layer midplane for the interdigitated pattern

In order to evaluate the effect of the flow channel pattern in current distribution, current density in the midplane of the cell was plotted. It was verified that the current in the interdigitated (Figure 9) pattern is better distributed when compared to the serpentine (Figure 8).
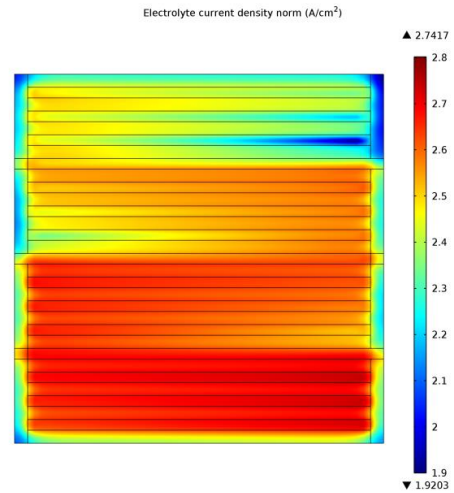


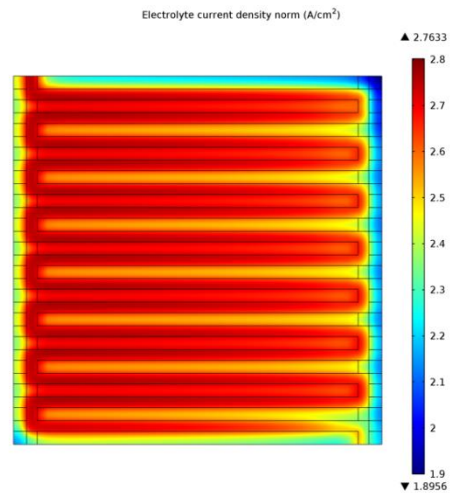**Figure 8.** Current density for the serpentine pattern



**Figure 9.** Current density for the interdigitated pattern

Current density close to the gas inlet is higher than that in the exit region, mainly for the serpentine pattern. As aforementioned, the reactant concentration decreases as they flow along the channels, and this behavior is followed by the reaction rate and resulting current.

This is evident in Figure 10, where $O_2$ consumption rate and channel pressure in the serpentine channel are plotted over the A-A cut. Because channels are intercalated with ribs along the length of the cut, the channel pressure curve is intermittent. Pressure and consumption rate is similar within every group of four channels. Additionally, more oxygen is consumed in the catalyst layer directly over channels, with a slight increase over the channel-rib boundary.
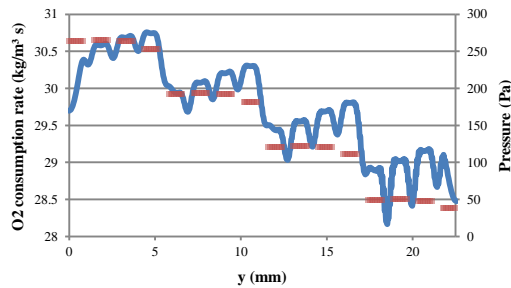
**Figure 10.** $O_2$ consumption rate (continuous blue) and channel pressure (intermittent red) over A-A for the serpentine pattern.

In the interdigitated pattern, the high-concentration gases are distributed to the channels connected to the inlet, while those connected to the outlet contain mostly depleted reactants. Therefore, the reaction rate is higher over the inlet channels than over the outlet channels. This is observed in Figure 11, where inlet and outlet channels can be clearly distinguished in the pressure plot. It is noteworthy that the pressure drop in the interdigitated pattern is higher than that in the serpentine. Also, in this pattern it is more noticeable that the reaction rate over the channel-rib boundary is highest, as concentrated reactant must flow through the porous layer in order to reach the outlet. Thus, current generation takes place in a well-defined but more dispersed area.
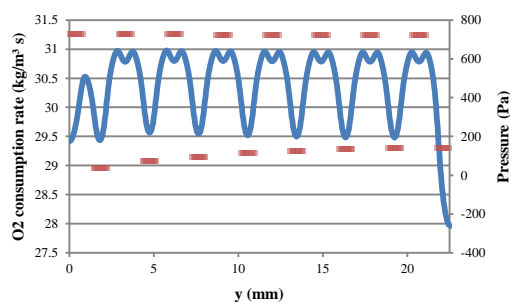


**Figure 11.** $O_2$ consumption rate (continuous blue) and channel pressure (intermittent red) over B-B for the interdigitated pattern.

## 5. Conclusions

Evaluating the current distribution of the fuel cell is an important tool for analyzing differences between different designs even when polarization curves show similar performances. In this study, it was clearly seen that the interdigitated pattern provides a more uniform current distribution throughout the MEA plane. A uniform heat generation can result in a better thermal management. In addition, in regions with different temperatures the cell may operate differently than specified, resulting in water management problems. Therefore, optimization of the flow channel pattern can lead to better fuel cell performances, and can lead to the choice of better fuel cell designs, particularly in scaled-up cases.

## 6. References

1. F. Barbir. *PEM Fuel Cells: Theory and Practice*. Academic Press, Burlington, MA, USA (2005)
2. Y. M. Ferng et al. A three-dimensional full-cell CFD model used to investigate the effects of different flow channel designs on PEMFC performance, *Int. J. Hydrogen Energy*, **32**, 4466-4476 (2007)
3. G. Hu et al. Three-dimensional numerical analysis of proton exchange membrane fuel cells (PEMFCs) with conventional and interdigitated flow fields, *J. Power Sources*, **136**, 1-9 (2004)
4. C. Spiegel. *PEM Fuel Cell Modeling and Simulation Using MATLAB®*. Academic Press, Burlington, MA, USA (2008)
5. W. Vielstich et al. (Ed.) *Handbook of Fuel Cells*. J. Wiley & Sons, New York, NY, USA (2003)
6. G. Doubek et al. Application of CFD techniques in the modeling and simulation of PBI PEMFC. *Fuel Cells*, **11**, 764-774 (2011)
7. E. Robalinho. *Desenvolvimento de um modelo numérico computacional aplicado a uma célula a combustível unitária de 144 cm² do tipo PEM.* PhD Thesis, São Paulo, SP, Brazil (2009)
8. M. Linardi. *Introdução à Ciência e Tecnologia de Células a Combustível*. Artliber Editora, São Paulo, SP, Brazil (2010)

## 6. Acknowledgements